

# NUMERICAL ANALYSIS OF MAGNETOHYDRODYNAMIC FLOW CHARACTERISTICS OF CU-WATER NANOFLUID PAST A WAVY VERTICAL PLATE-FINITE DIFFERENCE APPROACH

<sup>1</sup>Penthala Rajitha, <sup>2</sup>S Karunakar Reddy

[sar.telangana@gmail.com](mailto:sar.telangana@gmail.com)

[karunakarreddy.shadagonda@gmail.com](mailto:karunakarreddy.shadagonda@gmail.com)

<sup>1,2</sup> Assistant Professor, Department of Mathematics,  
St.Mary's Group of Institutions Hyderabad

## ABSTRACT

The finite difference approach is used in this work to numerically analyze the flow of a Cu-water nanofluid over a permeable vertical surface with a wavy design. Reynolds number ( $R$ ), nanoparticle volume fraction ( $\phi$ ), and magnetic field strength ( $M$ ) are the three main parameters that are examined in relation to the flow dynamics. A higher Reynolds number improves fluid motion and dramatically changes the velocity distribution along the undulating surface, according to the data. A greater volume proportion of nanoparticles ( $\phi$ ) raises the viscosity and thermal conductivity of the nanofluid, which significantly affects the flow characteristics. Furthermore, a magnetic field resists fluid motion by producing a Lorentz force, which modifies the velocity profile and affects the overall stability of the flow. These results have significant applications in industrial cooling technologies, biomedical engineering, and thermal management since they shed light on the behavior of magnetohydrodynamic nanofluid flows over intricate geometries.

**Keywords:** Nanofluid, Wavy flow, Reynolds number, Solid volume fraction, Magnetic field, MHD, Finite difference method.

## 1.INTRODUCTION

Nanofluids—suspensions of nanoscale particles in base fluids such as water, ethylene glycol, or oils—have garnered significant attention due to their superior thermal conductivity and potential to enhance heat and mass transfer in industrial and scientific applications. These fluids demonstrate notable improvements over traditional coolants in various sectors, including electronics, renewable energy, biomedical engineering, and manufacturing processes Koblinski et al., [1] and Saidur et al.,[2]. Their use in natural and forced convection systems offers opportunities for performance optimization in systems such as microchannels, heat exchangers, and high-power electronic cooling devices.

Studies by Sundar and Sharma [3] and Patel and Das [4] have demonstrated that the addition of metallic or metal oxide nanoparticles, including Cu, Al<sub>2</sub>O<sub>3</sub>, and TiO<sub>2</sub>, significantly enhances thermal conductivity while influencing the viscosity and flow stability of the host fluid. Recent developments have seen hybrid nanofluids, fluids containing more than one type of nanoparticle—emerge as a promising alternative due to synergistic effects that further boost heat transfer efficiency as per the studies by Sreedevi et al., [5]. Despite increasing exploration, comprehensive analysis of heat and mass transfer mechanisms involving

nanofluids over inclined and permeable surfaces remains limited. Wavy and vertical surfaces are particularly relevant in engineering configurations, including solar collectors, geothermal energy systems, and nuclear reactor walls. The interplay between buoyancy, fluid inertia, surface inclination, and the presence of nanoparticles creates a complex boundary layer structure that warrants deeper numerical and theoretical exploration in their works by Tiwari & Das [6]; Gorla & Chamkha, [7]. More recently, Niu et al. [8] numerically studied mixed convection heat transfer of hybrid nanofluids in vertical porous channels under the influence of variable magnetic fields and radiation. Their results highlighted the vital role of MHD forces in modulating the flow and thermal boundary layers. Likewise, the work of Hayat et al. [9] demonstrated that fluid rheology, Brownian motion, and thermophoresis effects governed by the Buongiorno model are crucial to accurately predict nanoparticle migration and energy transport in non-Newtonian nanofluid systems. Magneto hydrodynamics (MHD) offers another layer of complexity, especially in the presence of porous or permeable media. The application of magnetic fields can manipulate flow patterns through Lorentz forces, leading to drag reduction or thermal enhancement, depending on field orientation and strength as pointed by Sheikholeslami et al. [10]. In parallel, the role of surface suction and injection in controlling boundary layer thickness and delaying separation has been extensively reviewed by Rashidi et al. [11]. Advanced nanofluid models also incorporate temperature-dependent thermal conductivity, nanoparticle shape factor, and variable viscosity effects to reflect realistic engineering scenarios. For instance, the fractional calculus approach adopted by Khan et al. [12] and time dependent simulations conducted by Ali et al. [13] offer deeper insight into transient heat transfer phenomena and thermal stability of hybrid nanofluids.

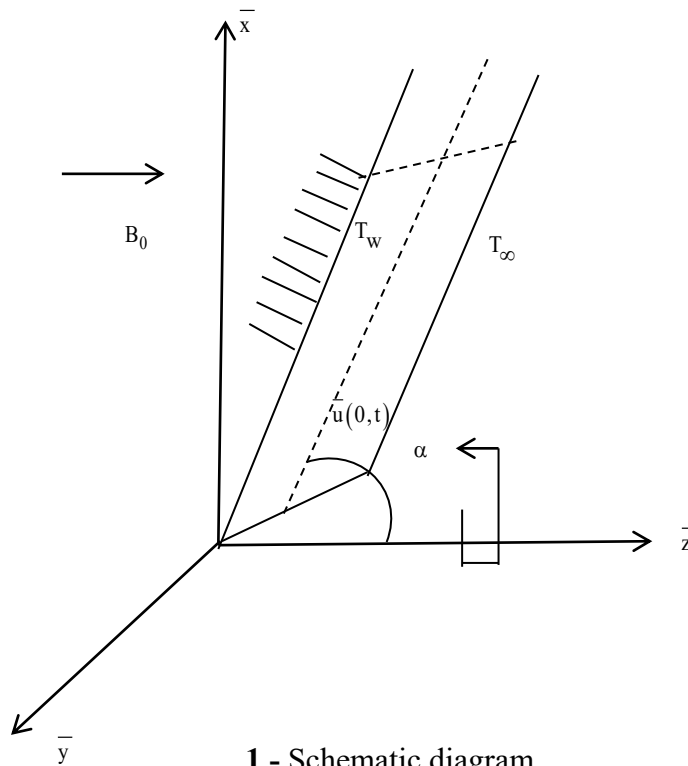
This paper focuses on investigating both free and forced convective heat transfer in a Cu-based nanofluid over a two-dimensional inclined vertical permeable surface. Using a finite difference method (FDM), the effects of critical parameters Reynolds number, nanoparticle volume fraction, surface inclination angle, and magnetic field intensity are analyzed in detail. The aim is to contribute a deeper understanding of nanofluid behavior in complex geometries, facilitating design optimization in cooling technologies and energy-efficient thermal systems.

## Mathematical Formulation

The main assumptions governing the flow with heat transfer is as follows:

- The unsteady convection flow of Copper-water Nano-fluids was considered in past vertical moving semi-infinite plate
- This plate was assumed to be non-electrically conducting and move in the positive  $z$ -direction with the velocity  $U_0$
- Here transverse magnetic field is applied
- Initially considering the electrically conducting fluid on the plate is at rest.
- Assuming that the induced magnetic field is smaller than the external magnetic field. By taking surface temperature as a constant value  $T_w$  and the ambient temperature as  $T_\infty$ , where  $T_w > T_\infty$
- Suppose that the regular fluid and suspended Cu particle are at the thermal equilibrium and no slip occurs between them
- The fluid was assumed to follow the Bossinesq approximation

The Cartesian co-ordinate system and also the geometry of the plate are shown in the following diagram.



1 - Schematic diagram

## 1. Governing Equations

The boundary layer equations governing the flow and temperature as per above assumptions are as follows

$$\frac{\partial u}{\partial x} + \frac{\partial v}{\partial y} = 0 \quad (1)$$

$$\rho_{nf} \left( \frac{\partial u}{\partial t} + u \frac{\partial u}{\partial x} + v \frac{\partial u}{\partial y} \right) = \mu_{nf} \left( \frac{\partial^2 u}{\partial x^2} + \frac{\partial^2 u}{\partial y^2} \right) - \sigma B_0^2 u \quad (2)$$

$$\rho_{nf} \left( \frac{\partial v}{\partial t} + u \frac{\partial v}{\partial x} + v \frac{\partial v}{\partial y} \right) = \mu_{nf} \left( \frac{\partial^2 v}{\partial x^2} + \frac{\partial^2 v}{\partial y^2} \right) \quad (3)$$

The boundary conditions for this problem are as follows:

$$u(x, y, 0) = 0, v(x, y, 0) = 0$$

$$u(0, y, t') = 0, v(0, y, t') = 0$$

$$u(x, 0, t') = x, v(x, 0, t') = 1$$

$$u(b, y, t') = 0, v\left(x, \frac{b}{2}, t'\right) = b + x, v\left(x, \frac{b}{2}, t'\right) = 0 \quad (4)$$

Thermo-Physical properties were related as follows:

$$\rho_{nf} = (1 - \phi)\rho_f + \phi\rho_s, \alpha_{nf} = \frac{k_{nf}}{(\rho c_p)_{nf}}$$

$$(\rho c_p)_{nf} = (1 - \phi)(\rho c_p)_f + \phi(\rho c_p)_s$$

$$(\rho\beta)_{nf} = (1 - \phi)(\rho\beta)_f + \phi(\rho\beta)_s$$

Here we introduce the following dimensionless variables as:

$$X = \frac{x}{L}, Y = \frac{y}{L}, t = t' \frac{U_0}{L}, U = \frac{u}{U_0}, V = \frac{v}{U_0} \quad (5)$$

Using equations (6), (7), (8) the equations (2), (3) & (4) can also be written in the following dimensionless form

$$\frac{\partial U(x, y, t)}{\partial t} + U(x, y, t) \frac{\partial U(x, y, t)}{\partial X} + V(x, y, t) \frac{\partial U(x, y, t)}{\partial Y} = \frac{1 + (2.5)\phi}{(1 - \phi + \phi \frac{\rho_s}{\rho_f})_R} \left( \frac{\partial^2 U(x, y, t)}{\partial X^2} + \frac{\partial^2 U(x, y, t)}{\partial Y^2} \right) - MU(x, y, t) \quad (6)$$

$$\begin{aligned} \frac{\partial V(x, y, t)}{\partial t} + U(x, y, t) \frac{\partial V(x, y, t)}{\partial X} + V(x, y, t) \frac{\partial V(x, y, t)}{\partial Y} \\ = \frac{1 + (2.5)\phi}{(1 - \phi + \phi(\frac{\rho_s}{\rho_f}))R} \left( \frac{\partial^2 V(x, y, t)}{\partial X^2} + \frac{\partial^2 V(x, y, t)}{\partial Y^2} \right) \end{aligned} \quad (7)$$

Here the corresponding boundary condition of equation (5) was written in the dimensionless form as:

$$\begin{aligned} U(x, y, 0) = 0, V(x, y, 0) = 0 \\ U(0, y, t) = 0, V(0, y, t) = \sin\left(\frac{\pi}{6}y\right) \\ U(x, 0, t) = x, V(x, 0, t) = 0 \\ U(b, y, t) = b, V\left(x, \frac{b}{2}, t\right) = b + x, V\left(x, \frac{b}{2}, t\right) = 0, V(b, y, t) = \frac{b}{2} + \sin\left(\frac{\pi}{6}\right)y \end{aligned} \quad (8)$$

Where the parameters present in the above equations are as follows:

$$Pr = \frac{\nu_f}{\alpha_f}, \text{ (Prandtl Number),}$$

$$M = \frac{\sigma B_0^2 L}{U_0 \rho_f}, \text{ (Magnetic field parameter),}$$

$$Re = \frac{LU_0}{\nu}, \text{ (Reynolds Number),}$$

### Solution of the Problem

The differential equations from (6) to (7) are nonlinear and coupled. The boundary conditions described in (8) were applied when solving these equations. The study is carried out in two dimensions over an infinite rectangular plate. For computational purposes, the domain is restricted to a finite region where the plate has a width of one unit and a height of two units. The system of equations is solved numerically using the "NDSolve" function in *Mathematica 10.4*, which efficiently handles nonlinear partial differential equations over bounded domains.

The Nusselt number (Nu), a dimensionless parameter that characterizes the local rate of convective heat transfer relative to conductive heat transfer across the boundary, is defined as:

$$Nu = -\frac{k_{nf}}{k_f} \theta'(0)$$

where  $\theta$  is the dimensionless temperature, and the derivative is evaluated at the surface of the plate (typically at  $y=0$ ).

### Discussion of the Results

The graphs in Figures 2 to 7 illustrate the effects of various governing parameters on the velocity components ( $u$  and  $v$ ) and temperature distribution ( $\theta$ ). These parameters include the Reynolds number ( $Re$ ), solid volume fraction ( $\phi$ ), magnetic parameter ( $M$ ). The Prandtl number ( $Pr$ ) was fixed at 0.7, corresponding to water. For consistency in spatial evaluation, horizontal velocity ( $v$ ) is measured at the cross-section  $x=1$ , while vertical velocity ( $u$ ) and temperature ( $\theta$ ) are evaluated at the mid-height of the domain,  $y=1/2$ .

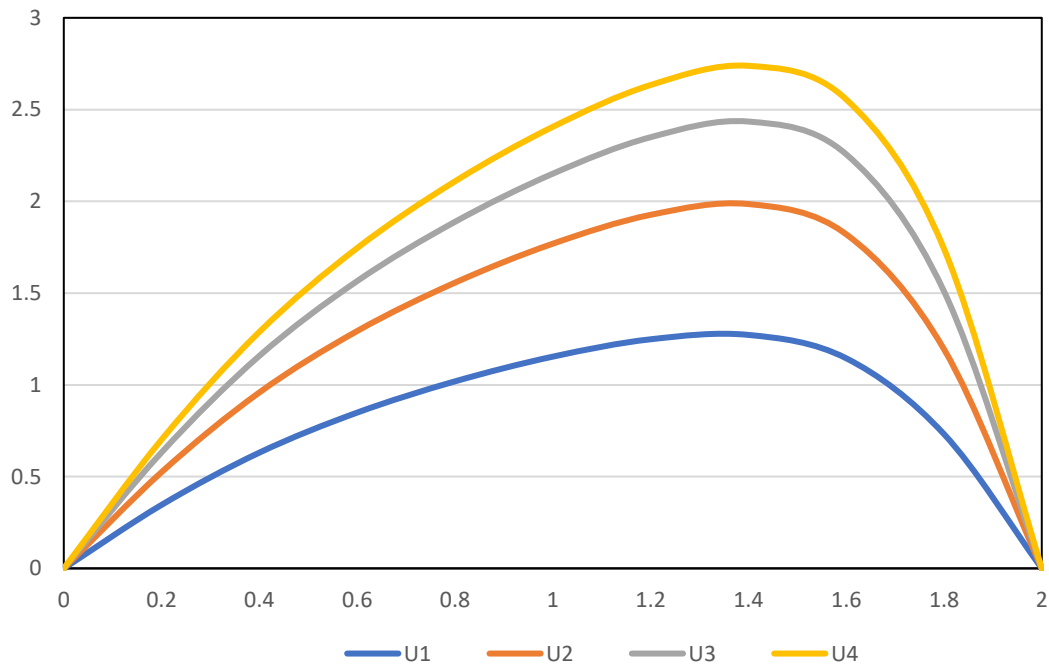
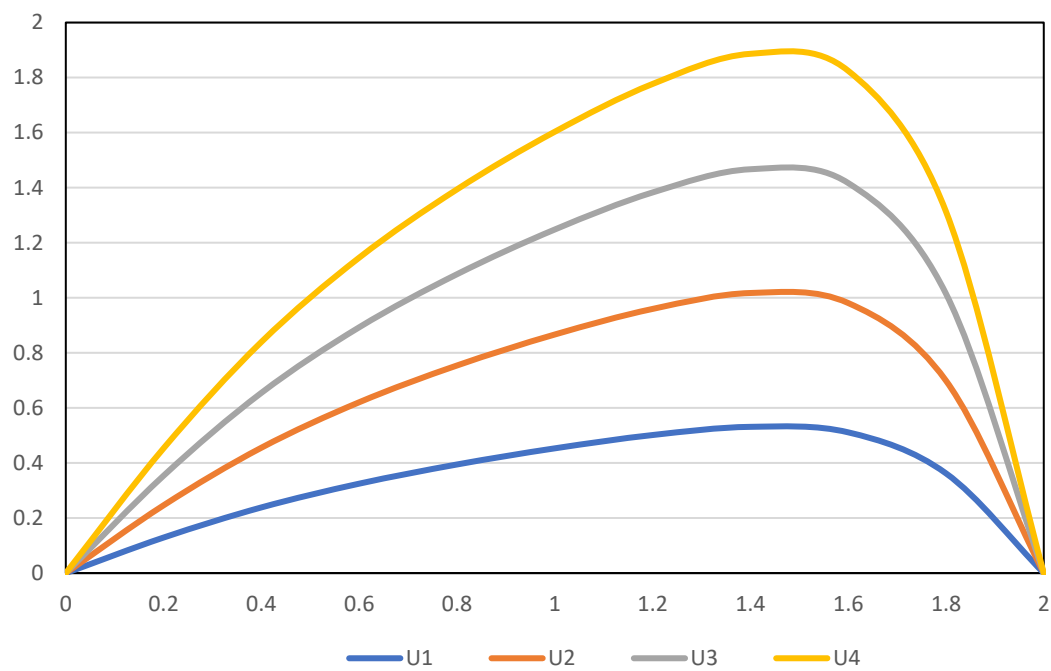
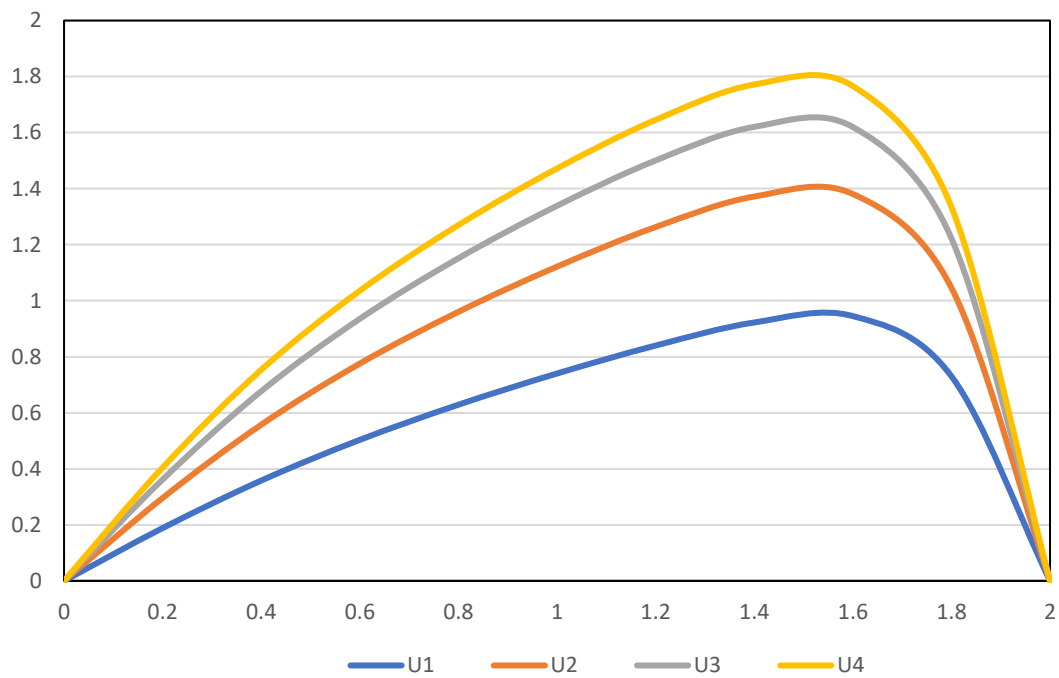


Fig.2. Profile of vertical velocity  $u$  with  $Re$



**Fig.3** Profile of vertical velocity  $u$  with  $\phi$



**Fig.4**Profile of vertical velocity u with M

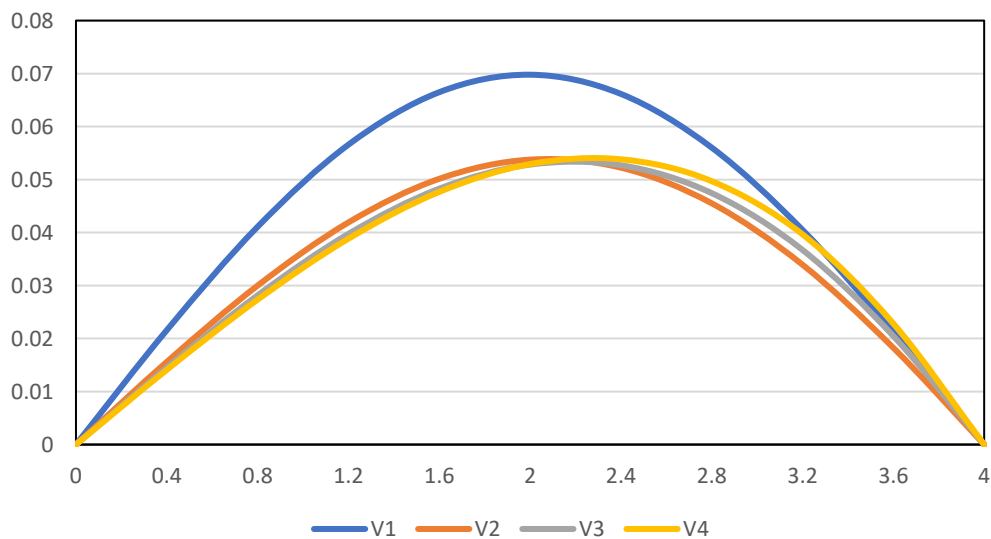


**Fig.5**Profile of v with Re

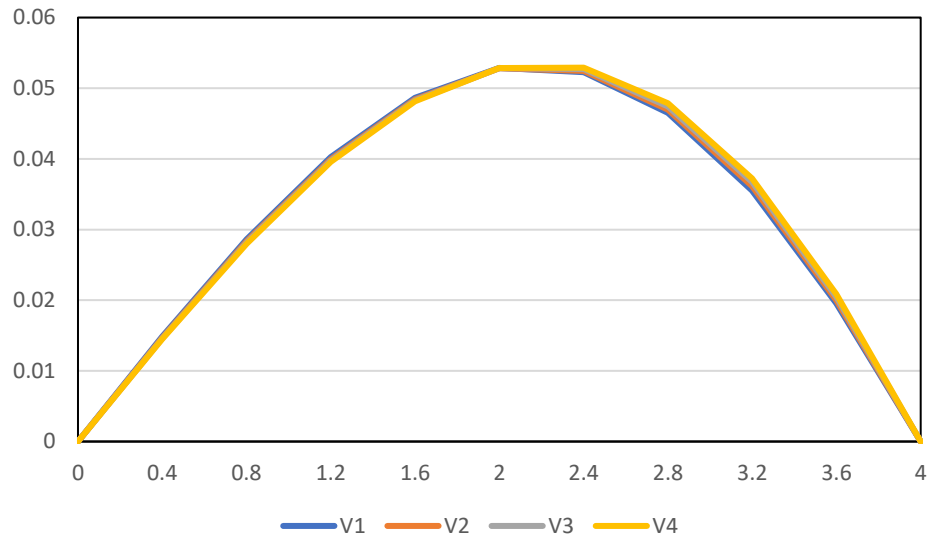


**Fig.6.** Profile of  $v$  with  $\phi$

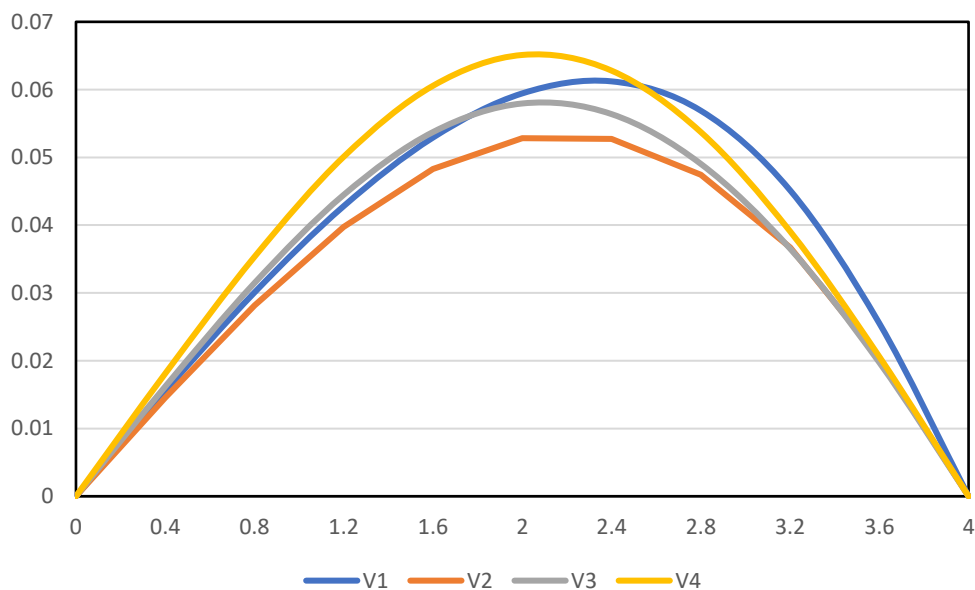


**Fig.7.** Profile of  $v$  with  $M$

Figures 2 through 4 illustrate the vertical velocity ( $u$ ) profiles for both natural and forced convection scenarios. Across all parameter variations, the vertical velocity is consistently greater in natural convection than in forced convection. This can be attributed to the buoyancy-driven nature of natural convection, where temperature gradients play a dominant role in initiating fluid motion. In contrast, forced convection relies heavily on external boundary movement to drive the flow. Specifically, in Fig. 2, the flow behavior demonstrates

a direct proportionality to the inertial force (represented by the Reynolds number,  $Re$ ) in natural convection, whereas in forced convection, it shows an inverse relationship. This indicates that increased inertial effects support natural convective flow but hinder forced convection when the plate movement governs the velocity field.

Fig. 5 highlights the impact of the solid volume fraction ( $\phi$ ), showing an inverse relationship with vertical velocity in both convection types. As the concentration of nanoparticles increases, the overall fluid viscosity increases, thereby resisting flow and reducing the vertical velocity. However, this retardation is observed to be gradual rather than abrupt. Fig. 4 indicates that the Lorentz force, introduced by the magnetic parameter ( $M$ ), plays a dominant role in suppressing the flow due to the electromagnetic damping effect, which is consistent in both convection types. In Fig. 6, the influence of the heat source parameter ( $Q_h$ ) on vertical flow appears to be minimal, but with increasing values, a slight negative impact is noted. This phenomenon is attributed to the presence of metallic nanoparticles (such as copper) that act as heat absorbers, thereby reducing the thermal buoyancy forces. Consequently, Cu-water nanofluids are particularly effective in systems where heat absorption is desired, such as in thermal regulation or heat-generating equipment.

Figures 7 focus on the horizontal velocity ( $v$ ) distribution. Similar to the vertical flow trends, natural convection exhibits higher horizontal velocity magnitudes than forced convection across all parameter variations. The horizontal flow is predominantly concentrated near the base of the plate and diminishes as one moves away from it, reflecting the influence of boundary-induced shear. Fig. 7 reveals that viscous forces overpower inertial forces at higher Reynolds numbers, leading to enhanced horizontal flow. Fig. 8 explores the effect of nanoparticle presence, particularly highlighting the role of Brownian motion in enhancing horizontal velocity in both convection modes. Interestingly, forced convection shows more pronounced sensitivity to these changes. The effect of the Lorentz force, which again suppresses velocity in both cases. However, the impact of the magnetic parameter ( $M$ ) appears less significant when compared to its influence on vertical velocity, suggesting anisotropy in magnetic damping depending on the flow direction.

## Conclusions

- Natural convection exhibits stronger vertical and horizontal velocity profiles than forced convection for all parameter variations, due to the dominance of buoyancy forces over boundary-driven flow. Key parameters such as Reynolds number, solid volume fraction, magnetic field strength, and plate inclination significantly affect the flow differently in each convection type.
- Cu-water nanofluids enhance horizontal velocity via Brownian motion but slightly reduce vertical flow due to their heat absorption capacity. The Lorentz force consistently suppresses flow in both directions, indicating its effectiveness in controlling convection in magnetohydrodynamic systems.

## References

- [1]. Keblinski, P., et al. (2002). *Mechanisms of heat flow in suspensions of nano-sized particles (nanofluids)*. International Journal of Heat and Mass Transfer, 45(4), 855–863.

- [2]. Saidur, R., et al. (2011). A review on applications and challenges of nanofluids. *Renewable and Sustainable Energy Reviews*, 15(3), 1646–1668.
- [3]. Sundar, L. S., & Sharma, K. V. (2015). A review of thermophysical properties of nanofluids. *Renewable and Sustainable Energy Reviews*, 43, 164–177.
- [4]. Patel, H. E., & Das, S. K. (2010). Experimental investigations on the thermal conductivity of Cu–Zn hybrid nanofluids. *International Communications in Heat and Mass Transfer*, 37(1), 82–86.
- [5]. Sreedevi, P., et al. (2019). Heat transfer analysis of hybrid nanofluids: A review. *Materials Today: Proceedings*, 18, 4545–4550.
- [6]. Tiwari, R. K., & Das, M. K. (2007). Heat transfer augmentation in a two-sided lid-driven differentially heated square cavity utilizing nanofluids. *International Journal of Heat and Mass Transfer*, 50(9-10), 2002–2018.
- [7]. Gorla, R. S. R., & Chamkha, A. J. (2011). Natural convection in a tilted square enclosure filled with nanofluid. *International Journal of Numerical Methods for Heat & Fluid Flow*, 21(5), 593–608.
- [8]. Niu, J., et al. (2021). MHD mixed convection of hybrid nanofluid in a porous vertical cavity under radiative effects. *Journal of Thermal Analysis and Calorimetry*, 143, 1053–1067.
- [9]. Hayat, T., et al. (2020). Impacts of thermophoresis and Brownian motion on the flow of hybrid nanofluid over a vertical plate. *Results in Physics*, 17, 103042.
- [10]. Sheikholeslami, M., et al. (2016). Numerical simulation of MHD nanofluid flow and heat transfer in a porous cavity using lattice Boltzmann method. *Journal of Molecular Liquids*, 221, 1014–1023.
- [11]. Rashidi, M. M., et al. (2014). The effect of thermal radiation and Joule heating on MHD flow over a stretching sheet using spectral local linearization method. *Journal of the Taiwan Institute of Chemical Engineers*, 45(3), 903–912.
- [12]. Khan, Z. H., et al. (2020). Fractional modeling of nanofluid flow over a stretching sheet with magnetic effects. *Alexandria Engineering Journal*, 59(3), 1295–1303.
- [13]. Ali, R., et al. (2022). Transient analysis of hybrid nanofluid flow under fractional derivative model. *Physica Scripta*, 97(6), 065205.